Exhumation History of the Alam Kuh Area, Central Alborz Mountains, Northern Iran: Implications for Caspian subsidence and Collision-Related Tectonics

Gary J. Axen, Patrick S. Lam, Marty Grove

Department of Earth and Space Sciences, University of California, Los Angeles

Daniel F. Stockli

Division of Geological and Planetary Sciences, California Institute of Technology, Pasadena

Jamshid Hassanzadeh

Institute of Geophysics, University of Tehran, Iran

Abstract. Crystallization and thermal histories of two plutons in the northwestern Alborz (also Elburz, Elburs) Mountains, northern Iran were obtained by U/Pb, $^{40}Ar/^{39}Ar$, and (U-Th)/He analyses of zircon, biotite, K-feldspar, and apatite. The Akapol granodiorite intruded at 56±2 Ma, cooled to ~150°C by ~40 Ma, and resided at that temperature until at least 25 Ma. The nearby Alam Kuh granite intruded at 6.8±0.1 Ma. It cooled rapidly to background temperatures (125-175°C) by 6 Ma. Persistence of ~150°C ambient conditions indicate tectonic stability for the Alam Kuh region from Late Eocene to Late Miocene time. Elevation-correlated (U-Th)/He ages from the Akapol suite indicate 0.7 km/m.y. exhumation between 6 and 4 Ma. This correlates well with the onset of coarse molasse deposition in the Zagros fold belt and accelerated sedimentation in the south Caspian Sea at ~6 Ma and suggests that all events represent a nearly instantaneous response to Arabian-Eurasian collision. Moreover ~10 km of subsidence in the Caspian basin may be attributed to loading by the Alborz Mountains. Steep, dextral northwest-trending strike-slip faults in the Alam Kuh region cut the Akapol granodiorite and are truncated by the Alam Kuh pluton. These results suggest that the change from Tertiary dextral strike-slip faulting to presently observed sinistral strike-slip may have occurred as late as 7 Ma, possibly due to the Late Neogene onset of continental collision.

INTRODUCTION

Iran represents the key locality on Earth to study upper crustal response to early processes of continental collision processes due to the Late Miocene-Recent collision between Arabia, Eurasia and intervening cratonal rocks underlying Iran (Fig. 1). The Arabian Peninsula is converging northward with respect to Eurasia at >20 cm/yr

(DeMets et al., 1990) and has formed the Bitlis-Zagros suture extending southeast from Turkey to the Persian Gulf. The collision began in late Miocene time (~12 Ma) in Turkey and progressed southeast (Dewey et al., 1973). Suturing has not yet occurred within the Gulf of Oman and the Makran, where subduction remains active.

The narrow mountain ranges separated by wide lowlands of central Iran distinguish it topographically from the broad, ca. 2000 m orogenic plateau that encompasses parts of Turkey, Iraq, and western Iran. The northernmost of these ranges, the rugged Alborz Mountains, extend laterally 900 km around the south Caspian Sea and are located 200-500 km north of the Neo-Tethyan suture (Fig. 1). The Alborz has an average elevation of nearly 3000 m and includes three of the highest points in Iran (the Quaternary Damavand volcano, 5670 m; Alam Kuh, 4822 m; and Takht-e-Soleiman, 4659 m). Elevation decreases abruptly northwards over ~50-60 km to the Caspian Sea (~30 m below sea level). The south Caspian, site of intense oil exploration, is possibly the deepest sedimentary basin in the world, with up to 20 km of Jurassic(?) and younger sediments overlying mafic basement (Neprochnov, 1968; Berberian, 1983; Devlin et al., 1999). Overall structural relief from the Alborz Mountains to the southernmost Caspian basement is ~25 km.

Few exposed intrusive rocks in the Alborz can be dated to establish the timing of faulting. However, in the Alam Kuh region, several plutons either truncate, or are cut by, faults representative of other strike-slip faults present throughout the central Alborz (Fig. 2). Moreover, steep glacial topography and strong local relief provide three-dimensional control that greatly benefits thermal history studies. We present here integrated U/Pb zircon, $^{40}Ar/^{39}Ar$ K-feldspar, and (U-Th)/He apatite thermal history results from a foliated intrusion (Akapol granodiorite) cut by strike-slip faults and an apparently undeformed body (Alam Kuh granite) that intrudes similar faults. Previously, these plutons were assigned ages ranging from Precambrian to Pleistocene based on regional relations (Gansser & Huber, 1962; Annells, 1977; Vahdati-Daneshmand, 1991). Our results permit us to determine the timing of strike-slip faulting and exhumation history of the Alam Kuh region and link these data to broader, Late Neogene tectonic processes that affected the region.

TECTONIC SETTING

Iran is underlain by an assemblage of microcontinents sandwiched between the converging Arabian and Eurasian cratons (McCall, 1998) (Fig. 1). The Indian craton presents a buttress hindering extrusion to the east. Closure of the Neo-Tethys ocean occurred by subduction in the region of the present Zagros Mountains (Fig. 1) (Stocklin, 1968; Berberian and King, 1981; Alavi, 1994). The Urumiyeh-Dokhtar magmatic arc (about 150 km

southwest of the Alam Kuh area) formed above this subduction zone and was active from early Cretaceous to Quaternary time with prolific magmatism during Eocene to Miocene (Alavi, 1994). The northern margin of the Arabian plate deformed to form the Zagros fold and thrust belt (Fig. 1) as collision took place (Alavi, 1994). The Latest Miocene-Pliocene onset of coarse clastic deposition in the Zagros fold belt presumably dates significant collision-related uplift in the suture zone (Dewey et al., 1973; Sengor, 1986; Beydoun et al., 1992). Simultaneously (~5 Ma), an order-of-magnitude increase in sedimentation rate occurred in the south Caspian basin, reaching a peak of ~1.2 km/m.y. in Pleistocene time (Nadirov et al., 1997).

Crustal thickness under Iran decreases northeastward from ~55 km beneath the Zagros Mountains to 35-40 km under the Alborz, and finally to ~30 km in the south Caspian Sea (Dehghani and Makris, 1984; Seber et al., 1997). Strongly attenuated upper-mantle seismic velocities (Kadinsky-Cade et al., 1981) and Quaternary volcanism (Berberian and King, 1981) suggest the presence of shallow, anomalously hot, partially molten mantle asthenosphere beneath northern Iran. Gravity anomalies which indicate an insufficient crustal root beneath the Alborz (Dehghani and Makris, 1984; Annells et al., 1975) suggest that this anomalous mantle supports the elevation of the Alborz. However, the Alborz may be partially flexurally supported by the Caspian lithosphere. Although plate-circuit models show north or north-northwest convergence between Arabia and Eurasia (DeMets et al., 1990), seismicity indicates active deformation within the Alborz is partitioned between range-parallel sinistral faults and range-perpendicular thrusting (Preistley et al., 1994 and references therein). Hence, motion along the latter moves the western Alborz mountains northeastward over the Caspian (Fig. 1).

The geology of the Alam Kuh area has been mapped at scales ranging from ~1:70,000 to 1:250,000 (e.g., Gansser and Huber, 1962; Annells et al., 1975; 1977; Vahdati-Daneshmand, 1991). Exposed in the range are late Precambrian to Jurassic sedimentary rocks, Cretaceous greenstone, and Paleocene-Eocene marine tuffs (Stocklin, 1974). Based upon observations made along the eastern and western margins of the Alborz range, Alavi (1996) has interpreted the Alborz range as consisting of a system imbricate thrust sheets. Low-angle, dip-slip thrusts are present in the study area, (e.g. Alamut Rud fault) and place Eocene volcanics over Neogene redbeds (Annells, 1977). However, our observations indicate high-angle, strike slip faulting is the most important type of deformation affecting the central Alborz. Key structural relationships in the Alam Kuh region include: (1) steep contacts of the Akapol pluton are dextrally offset 2-4 km by a previously unnamed fault zone (Barir fault zone Fig. 2). The Barir fault zone and the newly named Tang-e-Galu fault zone (Fig. 2) also display dextral kinematic indicators at outcrop

scale. Twenty-five kilometers to the northwest, Annells et al. (1975) map a pluton dextrally offset ~12 km by the Nusha fault. (2) Most faults in the Alam Kuh region dip moderately to steeply toward the core of the range, in a flower-structure geometry. (3) In range-perpendicular cross sections, most of these faults have reverse separation with a few indicating normal separation. The latter are consistent with motion in and out of the plane of section, as is common in transpressional systems. (4) Traced along strike, some fault zones, e.g., the Kandavan "overthrust" (Fig. 2) actually reverse dip and change sense of throw along strike (Vahdati-Daneshmand, 1991), again consistent with transpression.

METHODS

Concentrates of zircon, K-feldspar, biotite, and apatite were obtained from samples (Fig. 2) by standard magnetic and density techniques followed by hand selection under a binocular microscope. The UCLA Cameca ims 1270 ion microprobe was employed to measure U-Pb ages of epoxy-mounted zircons (Dalyrmple et al., 1999). Lead yields were enhanced by oxygen flooding (3×10^{-5} Torr) and a 4-18 nA, 25 μm primary O^- beam. Measurements of ^{208}Pb and ^{232}Th were used to correct for common Pb. Standard zircon AS-3 (1099 Ma) was employed to determine Pb/U relative sensitivity. Samples chosen for $^{40}Ar/^{39}Ar$ analysis were irradiated for 45 hours in the Ford Reactor (L67 position) using Fish Canyon sanidine (27.8±0.3 Ma) to monitor neutron fluence. Step-heating experiments were performed at UCLA in a Ta resistance furnace with the purified gas analyzed by a VG 1200S mass spectrometer (Lovera et al., 1997). Duplicate isothermal measurements were performed at low-temperature to generate the data necessary to correct $^{40}Ar^*/^{39}Ar_K$ for Cl-correlated excess ^{40}Ar (Harrison et al., 1994). K-feldspar results were interpreted using the multi-diffusion domain model (Lovera et al., 1997).

Apatite (U-Th)/He dating is based on the radiogenic production of ^4He from the decay of U and Th. On geologic time scales, He is completely expelled from apatite above ~80°C, partially retained between ~80-40°C, and totally retained below ~40°C (House et al., 1999; Farley, 2000). Assuming a constant cooling rate of 10°C/my, the (U-Th)/He thermochronometer has a bulk closure temperature of ~70°C. He determinations were carried out at Caltech using noble gas isotope dilution quadrupole mass spectrometry. U and Th concentrations of the same grains were determined by isotope dilution inductively coupled plasma mass spectrometry. Analytical uncertainties on age determinations are generally <6% (±2σ). The major limitation upon the accuracy of (U-Th)/He age determinations is the potential inclusion of zircon and monazite crystallites that cause irreproducible, anomalously old (U-Th)/He ages

(e.g., House et al., 1999). To mitigate against this, apatites were optically inspected prior to analysis to eliminate suspect grains and multiple experiments were run to determine age reproducibility of individual samples.

RESULTS

Results are summarized in Table 1[1]. Zircon U-Pb ages from three Akapol suite samples are adversely affected by low U contents and hence low radiogenic Pb (typically 50-60% radiogenic ^{206}Pb). Using anthropogenic lead compositions from the Los Angeles basin ($^{206}Pb/^{208}Pb = 0.474$; $^{207}Pb/^{208}Pb = 0.411$), we calculate a mean $^{206}Pb/^{238}U$ age for the three samples of 56 ± 2 Ma (1σ) which we interpret as the time of crystallization. Higher uranium content in zircon from the younger Alam Kuh sample (>1000 ppm) resulted in typically 95% radiogenic ^{206}Pb yields and essentially concordant $^{206}Pb/^{238}U$ and $^{207}Pb/^{235}U$ ages. The more precisely defined $^{206}Pb/^{238}U$ ages indicate a crystallization age of 6.8 ± 0.1 Ma (1σ).

Step-heating results from two biotite samples from the Akapol pluton yield weighted mean $^{40}Ar/^{39}Ar$ ages between 56-57 Ma, consistent with the U-Pb zircon results. The observed age concordance (Fig. 3) is consistent with emplacement at depths with ambient temperature < 350°C (McDougall and Harrison, 1999). K-feldspar thermal history results from the Akapol suite confirm this and also indicate subsequent cooling to ca. 150°C by 40 Ma (Fig. 3). As indicated, isothermal conditions near 150°C affected the Akapol pluton from 40 Ma to at least 25 Ma. In contrast, thermal history results from the younger Alam Kuh pluton show that it cooled to 125-175°C by 6 Ma. Concordance of the total gas K-feldspar and U-Pb zircon ages (Table 1) is consistent with field observations that indicate shallow emplacement of the Alam Kuh body. These include relatively fine-grained texture, common miarolitic cavities, and the presence of associated, mineralogically similar glassy dikes in surrounding country rocks (Gansser and Huber, 1962; P.S. Lam and G.J. Axen, unpublished mapping).

Six apatite samples from the Akapol granodiorite yield very reproducible (U-Th)/He ages clustering between 5.9 and 4.4 Ma indicating rapid cooling below 70°C. The (U-Th)/He ages generally correlate with elevation increasing from 4.4 Ma at 1800 m to 5.9 Ma at 2880 m, except for the highest sample (3250m) from the Akapol granodiorite which yields an age of 5.0 Ma (Fig. 3). Excluding the anomalous sample, these results indicate an exhumation rate of 0.7±0.1 km/m.y. This implies 18°C/Ma cooling given a near-surface geotherm of 25°C/km. Unfortunately, apatite analyses from the younger Alam Kuh granite yield irreproducible (U-Th)/He ages that predate

the crystallization age (Table 1). While we analyzed only grains in which we could not detect inclusions, most apatites from the Alam Kuh granite were of poor quality with abundant small zircon inclusions. Irreproducible and anomalously old ages point to He contribution from undetected U- and Th- bearing inclusions (e.g., House et al., 1999). Note that the youngest and most reproducible (U-Th)/He ages (8.1 to 7.5 Ma) from the Alam Kuh granite closely approach the U/Pb crystallization age (Fig. 3).

DISCUSSION

Our new thermal history constraints span a critical interval (Early Tertiary to Late Neogene) in the evolution of the central Alborz Mountains. Intrusion of the Akapol granodiorite (56±2 Ma) was coeval with the main phase of igneous activity within the Urumiyeh-Dokhtar magmatic arc. Subsequent cooling to ~150°C by 40 Ma may reflect exhumation and crustal deformation that caused Eocene unconformities in central Iran (Berberian and King, 1981). Similarly, the subsequent interval of tectonic quiescence implied by protracted cooling at ca. 150°C (Fig. 3) coincides with stable shelf sedimentation in central Iran (Berberian and King, 1981). We interpret our results to indicate that isothermal conditions (ca. 150°C) reflecting tectonic stability persisted in the vicinity of the central Alborz until the time of intrusion of the Alam Kuh granite at 6.8±0.1 Ma (Fig.3).

Elevation-correlated (U-Th)/He ages ranging from 6 to 4 Ma suggest that collision-related denudation in the central Alborz began about the time the Alam Kuh granite was intruded. Assuming a regional steady-state geotherm of about 25°C/km implies that as much as ~5-7 km exhumation may have occurred after 7 Ma. Taking the 4 km elevation of the Alborz range into account, the total Late Neogene uplift may approach 10 km. This is comparable to the amount and rate of subsidence that has taken place within the south Caspian Sea near Baku where the upper 10 km of sediment are <6 Ma old (Nadirov et al., 1997). Although similar data are not available for the southernmost Caspian adjacent to the Alborz range, a 20 km deep sedimentary trough is known to occur there (Berberian, 1983). Provided that a similar thickness of < 6 m.y. sediment was deposited in this trough, then 60%, or 15 km, of the observed structural relief between the high Alborz and the southernmost Caspain basement (25 km) could have developed in the late Neogene. This supports the notion that a component of Caspian subsidence can be attributed to loading by the Alborz Mountains. Moreover, the temporal coincidence between subsequent 6-4 m.y. cooling and exhumation in the Alborz Mountains, the commencement of rapid sedimentation in the adjacent south Caspian Sea

---

[1] Complete data tables for individual analyses, GSA Data Repository item 0000, are available on request from Documents Secretary, GSA, P.O. Box 9140, Boulder, CO 80301, editing@geosociety.org,

at ~ 6 Ma (Nadirov et al., 1997), and the latest Miocene-Pliocene outbreak of coarse-grained molasse sedimentation in the Zagros fold belt implies that these geographically widespread phenomena had a common cause (i.e., initiation of continental collision in Iran).

Finally, the 6.8 Ma U-Pb age obtained for the Alam Kuh granite may help constrain the timing of a fundamental change in fault kinematics in the central Alborz Mountains. Regional seismicity indicates that sinistral strike-slip faulting (Preistley et al., 1994) is currently active in the area. However, faults in the Alam Kuh area have accommodated significant dextral-reverse slip typical of a transpressional environment during the Tertiary. For example, the dextral Barir fault zone post-dates the ~56 Ma Akapol pluton and the dextral Tang-e-Galu fault zone is intruded by the ~6.8 Ma Alam Kuh granite (Fig. 2). The northwestern continuation of the Kandavan "overthrust," which we interpret as a dextral transpressional feature, is also shown intruded by the west margin of the Alam Kuh pluton (Annells et al.,1977). Moreover, dextral offsets along strike-slip faults have also been described east and west of the Alborz (Sengor, 1990 and references therein). The result from the Alam Kuh granite lead us to conclude that the transition from dextral slip to sinistral slip along strike-slip faults in the Alam Kuh area reflects the regional Late Neogene tectonic change from subduction to continental collision and may relate to regional eastward extrusion of central Iranian microplates toward India (Fig 1).

Acknowledgements

We thank M. Mashaiekhi, E. Mashaiekhi, A. Sharifi, and B. Bashukooh for valuable assistance in the field and H. Beshavarpour for collecting sample 19-31-1. C.D. Coath assisted with the ion microprobe measurements. Aspects of this study were supported by NSF (Axen; EAR 9902932), the UCLA Academic Senate Council on Research (Axen), the Tehran University Research Council (Hassanzadeh; 651/1/328), the DoE (T.M. Harrison; DE-FG-03-89ER14049), a Caltech postdoctoral fellowship (Stockli), and a D. and L. Packard Foundation fellowship (K.A. Farley).

REFERENCES CITED

Alavi, M., 1994, Tectonics of the Zagros orogenic belt of Iran: new data and interpretations: Tectonophysics, v. 229, p. 211-238.

Alavi, M., 1996, Tectonostratigraphic synthesis and structural style of the Alborz mountain system in northern Iran: Journal of Geodynamics, v. 21, p. 1-33.

Annells, R.N., Arthurton, R.S., Bazley, R.A., and Davies, R.G., 1975, Explanatory text of the Qazvin and Rasht quadrangles map: Geological Survey of Iran, 94 p.

Annells, R.N., Arthurton, R.S., Bazley, R.A., Davies, R.G., Hamedi, M.A.R., and Rahimzadeh, F., 1977, Geological map of Iran, Shakran sheet 6162: Geological Survey of Iran, scale 1:100,000, 1 sheet.

Beydoun, Z.R., Clarke, M.W.H, and Stoneley, R., 1992, Petroleum in Zagros Basin: A Late Tertiary foreland basin overprinted onto the outer edge of a vast hydrocarbon-rich Paleozoic-Mesozoic passive-margin shelf, *in* Macqueen, R.W., and Leckie, D.A., eds., Foreland Basins and Fold Belts: The American Association of Petroleum Geologists, p. 309-339.

Berberian, M., and King, G.C.P., 1981, Towards a paleogeography and tectonic evolution of Iran: Canadian Journal of Earth Sciences, v. 18, p. 210-265.

Berberian, M., 1983, The Southern Caspian: A compressional depression floored by a trapped, modified oceanic crust: Canadian Journal of Earth Sciences, v. 20, p. 163-183.

Berberian, M., Jackson, J.A., Qorashi, M., Khatib, M.M., Priestley, K., Talebian, M., and Ghafuri-Ashtiani, M., 1999, The 1997 May 10 Zirkuh (Qa'enat) earthquake (M_w 7.2): faulting along the Sistan suture zone of eastern Iran: Geophysical Journal International, v. 136, p. 671-694.

Dalrymple, G.B., Grove, M., Lovera, O.M., Harrison, T.M., Hulen, J.B., Lanphere, M.A., 1999, Age and thermal history of the Geysers plutonic complex (felsite unit), Geysers geothermal field, California: a $^{40}Ar/^{39}Ar$ and U-Pb study: Earth and Planetary Science Letters, v. 173, p. 285-298.

Dehghani, G.A., and Makris, J., 1984, The gravity field and crustal structure of Iran: Neue Jahrbuch fur Geologische und Palaontische Abhandlungen, v. 168, p. 215-229.

DeMets, C., Gordon, R.G., Argus, D.F., and Stein, S., 1990, Current plate motions: International Journal of Geophysics, v. 101, p. 425-478.

Devlin, W.J., Cogswell, J.M., Gaskins, G.M., Isaksen, G.H., Pitcher, D.M., Puls, D.P., Stanley, K.O., and Wall, G.R.T., 1999, South Caspian Basin: Young Cool, and Full of Promise: GSA Today, v. 9, p. 1-9.

Dewey, J.F., Pitman, III, W.C., Ryan, W.B.F., and Bonnin, J., 1973, Plate tectonics and evolution of the Alpine system: Geological Society of America Bulletin, v. 84, p. 3137-3180.

Farley, K. A., 2000, Helium diffusion from apatite; general behavior as illustrated by Durango fluorapatite: Journal of Geophysical Research, v. 105, p. 2903-2914.

Gansser, A., and Huber, H., 1962, Geological Observations in the Central Elburz, Iran: Schweizerische Mineralogische und Petrographische Mitteilungen, v. 42(2), p. 583-630.

Harrison, T.M., Heizler, M.T., Lovera, O.M., Wenji, C., Grove, M., 1994, A chlorine disinfectant for excess argon released from K-feldspar during step-heating: Earth and Planetary Science Letters, v. 123, p. 95-104.

House, M.A., Farley, K.A., and Kohn, B.P., 1999, An empirical test of helium diffusion in apatite: borehole data from the Otway Basin, Australia. Earth and Planetary Science Letters, v. 170, p. 463-474.

Kadinsky-Cade, K., Barazangi, M., Oliver, J., Isacks, B., 1981, Lateral variations of high-frequency seismic wave propagation at regional distances across the Turkish and Iranian plateaus: Journal of Geophysical Research, v. 86, p. 9377-9396.

Lovera, O.M., Grove, M., Harrison, T.M., Mahon, K.I., 1997, Systematic analysis of K-feldspar $^{40}Ar/^{39}Ar$ step heating results, I, Significance of activation energy determinations: Geochimica et Cosmochimica Acta, v. 61, p. 3171-3192.

McCall, G.J.H., 1998, The geotectonic history of the Makran and adjacent areas of southern Iran: Journal of Asian Earth Sciences, v. 15, p. 517-531.

McDougall, I., and Harrison, T.M., 1999, Geochronology and Thermochronology by the $^{40}Ar/^{39}Ar$ method, 2nd ed.: New York, Oxford University Press, 269 p.

Nadirov, R.S., Bagirov, E., and Tagiyev, M., 1997, Flexural plate subsidence, sedimentation rates, and structural development of the super-deep South Caspian Basin: Marine and Petroleum Geology, v. 14, no. 4, p. 383-400.

Neprochnov, Yu.P., 1968, Structure of the earth's crust of epi-continental seas: Caspian, Black, and Mediterranean: Canadian Journal of Earth Sciences, v. 5, p. 1037-1043.

Priestley, K., Baker, C., Jackson, J., 1994, Implications of earthquake focal mechanism data for the active tectonics of the south Caspian Basin and surrounding regions: Geophysical Journal International, v. 118, p. 111-141.

Seber, D., Vallvé, M., Sandvol, E., Steer, D., and Barazangi, M., 1997, Middle East tectonics: applications of geographic information systems (GIS): GSA Today, v. 7, no. 2, p. 1-6.

Sengor, A.M.C., 1986, The dual nature of the Alpine-Himalayan system: Progress, problems and prospects: Tectonophysics, v. 127, p. 177-195.

Sengor, A.M.C., 1990, A new model for the Late Paleozoic-Mesozoic tectonic evolution of Iran and implications for Oman, *in* Robertson, A.H.F., Searle, M.P., and Ries, A.C., eds., The Geology and Tectonics of the Oman Region: Geological Society of London Special Publication no. 49, p. 797-831.

Stöcklin, J., 1968, Structural history and tectonics of Iran: a review: American Association of Petroleum Geologists Bulletin, v. 52, p. 1229-1258.

Stöcklin, J., 1974, Possible ancient continental margins in Iran, *in* Burk, C.A., and Drake, C.L., eds., The Geology of Continental Margins: New York, Springer-Verlag, p. 873-887.

Vahdati-Daneshmand, F., 1991, Amol; Geological quadrangle map of Iran: Geological Survey of Iran, scale 1:250,000, 1 sheet.

FIGURE CAPTIONS

Figure 1. Regional tectonic map of Iran and surrounding regions (after Alavi, 1994; Berberian et al., 1999): A, Ankara; B, Baku; D, Damavand Volcano; E, East Anatolian Fault; GC, Greater Caucasus; HK, Hindu Kush; KD, Kopet Dagh; LC, Lesser Caucasus; M, Mediterranean Sea; NAF, North Anatolian Fault; O, Gulf of Oman; SS, Sistan suture; T, Tehran.

Figure 2. Map of Alam Kuh region showing sample localities and faults (after Annells et al. 1975, Vahdati-Daneshmand 1991, Lam & Axen unpublished): A, Akapol pluton; AK, Alam Kuh pluton; BFZ, Barir fault zone; D, Dextral kinematic indicators on fault; KO, Kandevan "Overthrust"; AR, Alamut Rud thrust; TGFZ, Tang-e-Galu fault zone. Sedimentary country rock: Cz, Cenozoic; Mz, Mesozoic; Pz, Paleozoic; PC, Precambrian.

Figure 3. Thermal history results for the Alam Kuh region. Open symbols for Alam Kuh pluton; closed symbols for Akapol pluton. Zircon crystallization ages interpreted from U-Pb results (Table 1). Biotite bulk closure from total gas ages in Table 1 and Ar kinetics (McDougall and Harrison, 1999). K-feldspar thermal histories calculated as discussed in text. Bold lines indicate portions of thermal history constrained by ^{39}Ar release below melting. Apatite bulk He closure based upon total gas ages in Table 1, 18°C/m.y. cooling, ca. 50 μm radius, and He diffusion properties (Farley, 2000). Inset shows (U-Th)/He age vs. elevation basis for estimating exhumation rate. Data from 19-106-3 omitted. Alam Kuh apatites yield anomalously old (U-Th)/He ages due to minute zircon inclusions. See text for additional details.

TABLE 1. SUMMARY OF AGES FOR THE ALAM KUH AREA, NORTHERN IRAN

Sample	Location Latitude/Longitude (North/East)	Zircon * Pb/U ± 1σ (Ma)	Biotite † $^{40}Ar/^{39}Ar$ ± 1σ (Ma)	K feldspar§ $^{40}Ar/^{39}Ar$ ± 1σ (Ma)	Apatite (U-Th)/He ± 2σ (Ma)	Elevation (m)	Rock Type
Alam Kuh (AK) Suite							
19-29-1	36°22'41"/050°58'09"	6.8 ± 0.1			7.6 ± 0.5	4195	granite w/ miarolitic cavities
97AK104	36°22'41"/050°58'09"			6.8 ± 0.1	21 ± 1#	4195	granite w/ miarolitic cavities
19-31-1	36°22'34"/050°57'35"				8.1 ± 0.7	4600 ± 50	granite w/ miarolitic cavities
19-80-1	36°22'27"/050°57'18"				20 ± 1#	4620	granite w/ miarolitic cavities
19-79-2	36°22'32"/050°57'44"				7.5 ± 0.5	4880	granite w/ miarolitic cavities
Akapol Suite							
97AK102	36°26'38"/051°03'54"	56 ± 2	56.8 ± 0.1		4.4 ± 0.2	1800	foliated granodiorite
19-9-1	36°26'33"/051°03'58"				4.9 ± 0.2	1900	foliated granodiorite
97AK103	36°25'54"/051°02'30"		56.0 ± 0.1	51.9 ± 0.4	4.8 ± 0.2	2150	foliated granodiorite
19-12-1	36°24'40"/051°05'32"	54 ± 4				2620	rapikivi granite
97AK101	36°24'11"/051°02'35"	58 ± 3				2650	rapikivi granite
19-106-1	36°25'17"/051°00'46"				5.8 ± 0.3	2720	granodiorite
19-106-2	36°24'58"/051°00'37"				5.9 ± 0.3	2880	granodiorite
19-106-3	36°24'33"/051°00'34"				5.0 ± 0.3	3250	granodiorite

* Weighted mean age.

† Total gas age.

§ Total gas age corrected for Cl-correlated excess ^{40}Ar (Harrison et al., 1994).

Apparent (U/Th)/He ages with excess He derived from included zircon.

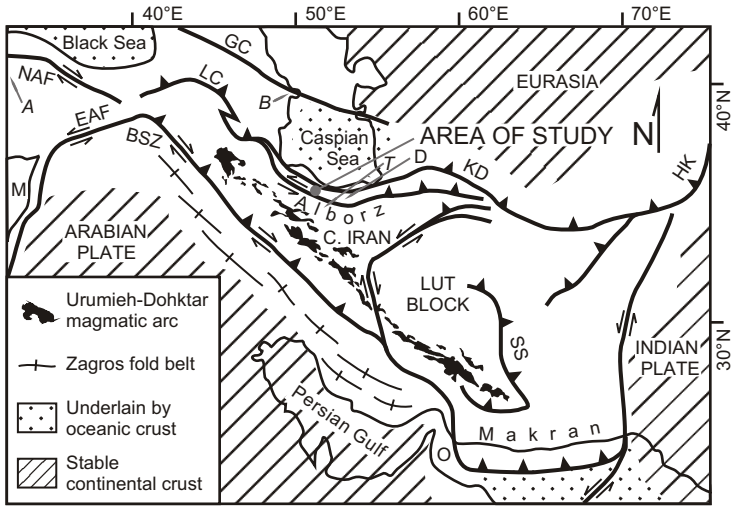
40°E
50°E
60°E
70°E
40°N
30°N
Black Sea
GC
NAF
A
LC
B
EAF
BSZ
EURASIA
AREA OF STUDY
N
Caspian Sea
T
D
KD
HK
M
Alborz
C. IRAN
ARABIAN PLATE
LUT BLOCK
SS
INDIAN PLATE
Persian Gulf
O
Makran
Urumieh-Dohktar magmatic arc
Zagros fold belt
Underlain by oceanic crust
Stable continental crust

Figure 1

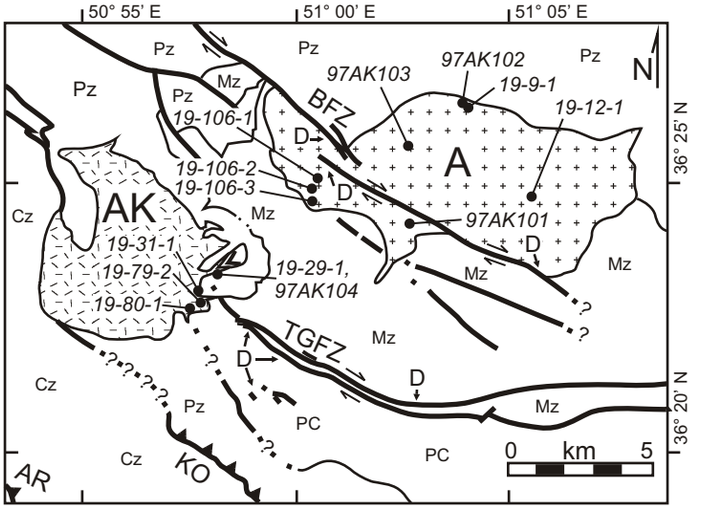
50° 55' E
51° 00' E
51° 05' E
36° 25' N
36° 20' N
N
Pz
Mz
Cz
PC
AK
A
AR
KO
BFZ
TGFZ
D
97AK103
97AK102
19-9-1
19-12-1
19-106-1
19-106-2
19-106-3
97AK101
19-31-1
19-79-2
19-80-1
19-29-1,
97AK104
0 km 5

Figure 2

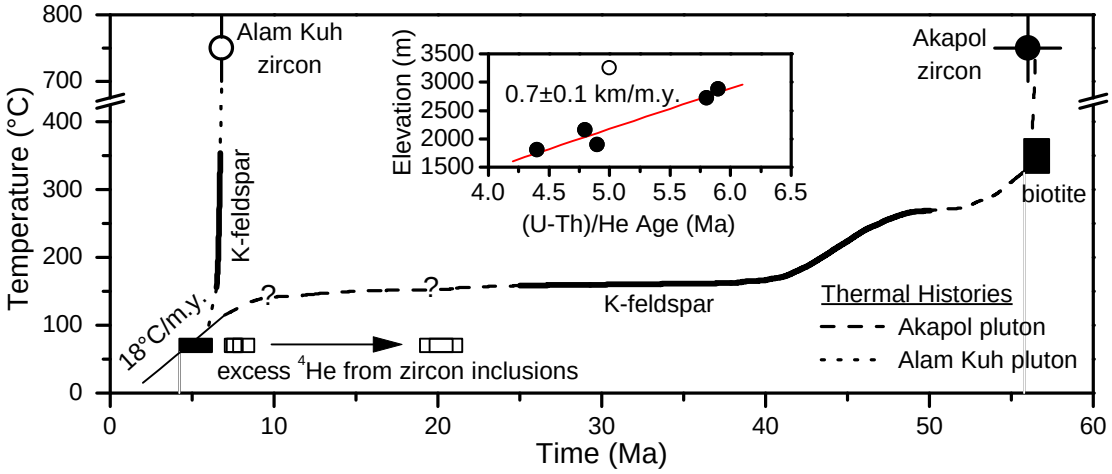
Temperature (°C)
Time (Ma)
Alam Kuh
zircon
K-feldspar
18°C/m.y.
?
?
K-feldspar
excess ^{4}He from zircon inclusions
Akapol
zircon
biotite
Elevation (m)
0.7±0.1 km/m.y.
(U-Th)/He Age (Ma)
Thermal Histories
Akapol pluton
Alam Kuh pluton

Figure 3